Liquid Crystals
Publication details, including instructions for authors and subscription information:
http://www.informaworld.com/smpp/title~content=t713926090

Synthesis and mesomorphic properties of chiral swallow-tailed thioester liquid crystals with lateral substituents

Shune-Long Wu[a]; Kuan-Ting Chen[a]
[a] Department of Chemical Engineering, Tatung University, Taipei, Taiwan, 104, ROC

To cite this Article Wu, Shune-Long and Chen, Kuan-Ting(2006) 'Synthesis and mesomorphic properties of chiral swallow-tailed thioester liquid crystals with lateral substituents', Liquid Crystals, 33: 5, 573 — 579
To link to this Article: DOI: 10.1080/02678290600605020
URL: http://dx.doi.org/10.1080/02678290600605020

Liquid Crystals, Vol. 33, No. 5, May 2006, 573–579

Synthesis and mesomorphic properties of chiral swallow-tailed thioester liquid crystals with lateral substituents

SHUNE-LONG WU* and KUAN-TING CHEN

Department of Chemical Engineering, Tatung University, 40 Chungshan N. Rd., 3rd Sec., Taipei, 104, Taiwan, ROC

(*Received 29 September 2005; accepted 30 December 2005*)

Two homologous series of chiral swallow-tailed thioester materials, 1-ethylpropyl (*R*)-2-[3-fluoro-4-(4′-alkyloxybiphenylcarbonylthio)phenoxy]propionates, I-6 (*m*=8–12), and 1-ethylpropyl (*R*)-2-[3-methyl-4-(4′-alkyloxybiphenylcarbonylthio)phenoxy]propionates, II-6 (*m*=8–12), have been synthesized and their mesomorphic phases studied. The results show that materials I-6 (*m*=8–12) with a fluoro substituent, display the phase sequence I–BPII–N*–SmC*–Cr, whereas materials II-6 (*m*=8–12) with a methyl substituent display the phase sequence I–N*–TGBA*–SmA*–Cr during cooling. The physical properties of the SmC* phase in materials I-6 were measured. The results show that the maximum $\mathbf{P}_s$ values are in the range 91–95 nC cm^{-2} and the maximum tilt angles are about 34–37°.

1. Introduction

The thioester group is well known to enhance mesophase ranges and mesophase thermal stabilities when compared with the ester group [1–5]. Neubert *et al.* reported that materials with the thioester group promoted the formation of smectic phases with wider temperature ranges [6]. Okamoto *et al.* reported a series of thioester liquid crystals with some lateral substituents [7]. Their results showed that the lateral substituents could reduce phase transition temperatures; they concluded that lateral substitution nearly always reduces smectic phase stability more than nematic phase stability because it is particularly disruptive to the lamellar packing for smectic phases [8].

Our recent study showed that the chiral swallow-tailed materials, 1-ethylpropyl (*R*)-2-[4-(4′-alkoxybiphenylcarbonyloxy)phenoxy]propionates, EP*m*PBPP (*m*=8–12), display a ferroelectric SmC* phase close to room temperature [9]. Thus, in order to obtain chiral liquid crystals whose SmC* phase encompasses room temperature, two series of chiral swallow-tailed thioester liquid crystals, I-6 (*m*=8–12) and II-6 (*m*=8–12), with fluoro and methyl substituents positioned at the 3-position of the phenyl ring, were designed and synthesized for investigation of their mesomorphic phases and electro-optical properties, The designed molecules have the general formula as shown below.

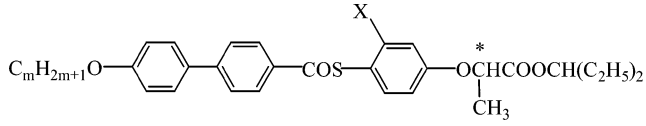

I-6: (m=8-12, X=F)
II-6: (m=8-12, X=CH_3)

2. Experimental

2.1. *Characterization of materials*

The structures of the intermediates and final products were identified by nuclear magnetic resonance spectroscopy using a Bruker Avance 500 NMR spectrometer. The purity of the final products was confirmed by elemental analysis using a Perkin-Elmer 2400 instrument. The carbon and hydrogen analytical data agreed with calculated results within ±1%.

Phase transition temperatures and enthalpy changes were determined by differential scanning calorimetry (DSC) using a Perkin-Elmer DSC 7 at a running rate of 5°C min^{-1}. Mesophases were identified using a Nikon Microphot-FXA polarizing optical microscope in conjunction with a Mettler FP82-HT hot stage controlled by a Mettler FP90 processor.

Commercial homogenous cells coated with polyimide as alignment film were purchased from E.H.C. Co. Ltd, Japan and Linkam Scientific Instruments Ltd, UK. Samples were filled into the cells by capillary action in the isotropic state. Two wires were fixed separately to the ITO-coated glass plates of sample cells with silver paint.

*Corresponding author. Email: slwu@ttu.edu.tw

Liquid Crystals
ISSN 0267-8292 print/ISSN 1366-5855 online © 2006 Taylor & Francis
http://www.tandf.co.uk/journals
DOI: 10.1080/02678290600605020

Spontaneous polarization ($\mathbf{P}_s$) was measured by the triangular wave method [10]. Triangular waves were generated by a Yogawa AG1200 arbitrary waveform generator and were amplified by an NF Electronics Instrument 4005 power amplifier. The currents were measured by detecting the voltage change across a resistor of 50 kΩ, using a HP 54502A digital oscilloscope to monitor the signals.

2.2. *Preparation of materials*

The starting chiral material, (*S*)-lactic acid, was purchased from Fluka Chem Co. Japan, with purity greater than 99%. Thin layer chromatography was performed with TLC sheets coated with silica; spots were detected by UV irradiation. Silica gel (MN kieselgel 60, 70–230mesh) was used for column chromatography. The organic solvent dichloromethane (CH_2Cl_2) and tetrahydrofuran (THF),were purified by treatment with CaH_2 and $LiAlH_4$, respectively, and distilled before use.

Some intermediates in scheme 1 were prepared according to conventional methods. Detailed synthetic procedures for other new intermediates and target materials are described below.

2.2.1. 3-Fluoro-4-thiocyanatophenol, I-2 [7]. The thiocyanation of phenol was carried out according to a previously described method [7]. A solution of *N*-chlorosuccinimide (15.49 g, 116 mmol) and ammonium thiocyanate (8.8 g, 116 mmol) in methanol (150 ml) was cooled at 0°C for 2 h. 3-Fluorophenol (6.5 g, 57.8 mmol) in methanol (50 ml) was added dropwise, and the mixture stirred at 0°C for 24 h. To the reaction mixture, a 20% aqueous solution of sodium hydrogen carbonate (200 ml) was added, and the precipitates were filtered off. Half of the filtrate solvent was evaporated *in vacuo*, and the residue was extracted twice with ether (50 ml). The combined ether layers were washed with water and dried over anhydrous magnesium sulphate. After removing the solvent, the residue was purified by column chromatography on silica gel (70–230 mesh) using dichloromethane as eluant. The product was recrystallized from a mixed ether/hexane solvent to give 3-fluoro-4-thiocyanatophenol as colourless needles; yield 15%, m.p. 66–68°C. ^{1}H NMR ($CDCl_3$): δ (ppm): 5.30 (br, 1H, O**H**), 6.56–6.62 (m, 2H, Ar**H**), 7.31–7.34 (t, 1H, Ar**H**, J=8.5 Hz).

2.2.2. 3-Methyl-4-thiocyanatophenol, II-2 [7]. The synthetic procedures for compound II-2 were similar to compound I-2. The product was obtained as colourless needles; yield 37%, m.p. 72–74°C. ^{1}H NMR ($CDCl_3$): δ (ppm): 2.49 (s, 3H, Ar**CH**$_3$), 5.43 (br, 1H, O**H**), 6.70–6.73 (dd, 1H, Ar**H**, J=8.5, 2.8 Hz), 6.80 (d, 1H, Ar**H**, J=2.6 Hz), 7.47–7.49 (d, 1H, Ar**H**, J=8.5 Hz).

2.2.3. 1-Ethylpropyl (*S*)-2-hydroxypropanoate, I-3. A solution of (*S*)-lactic acid (5 g, 55 mmol) and 3-pentanol (4.9 g, 55 mmol) in dry benzene (30 ml) was heated under reflux in a Dean and Stark trap for 10 h. Benzene was evaporated *in vacou*, and the residue distilled at low pressure. A colourless liquid was collected; yield 33%. ^{1}H NMR ($CDCl_3$): δ (ppm): 0.88–0.96 (m, 6H, CH(CH_2C**H**$_3$)$_2$), 1.42–1.44 (d, 3H, C*HC**H**$_3$, J=7 Hz), 1.58–1.62 (m, 4H, CH(C**H**$_2$CH$_3$)$_2$), 2.88 (s, 1H, O**H**), 4.24–4.28 (q, 1H, C***H**COO, J=6.8 Hz), 4.82–4.87 (m, 1H, COOC**H**).

2.2.4. 1-Ethylpropyl (*R*)-2-(3-fluoro-4-thiocyanatophenoxy)propionate, I-4 [11]. A solution of compound I-2 (1.58 g, 9.4 mmol), diethyl azodicarboxylate (DEAD, 1.63 g, 9.4 mmol) and triphenyl phosphine (Ph_3P, 2.45 g, 9.4 mmol) in anhydrous THF (20 ml) was stirred at 0°C. The compound I-3 (1 g, 6.2 mmol) was added dropwise to this solution, and the resulting mixture stirred for 24 h at room temperature. The solvent was evaporated *in vacuo*, and the residue purified by column chromatography on silica gel using dichloromethane/hexane (1/2) as eluant. The product was a yellow oil; yield 64%. ^{1}H NMR ($CDCl_3$): δ (ppm): 0.74–0.91 (m, 6H, CH(CH_2C**H**$_3$)$_2$), 1.50–1.60 (m, 4H, CH(C**H**$_2$CH$_3$)$_2$),1.63–1.64 (d, 3H, C*HC**H**$_3$, J=6.8 Hz), 4.70–4.74 (q, 1H, C***H**COO, J=6.8 Hz), 4.79–4.84 (m, 1H, COOC**H**), 6.60–6.63 (m, 2H, Ar**H**), 7.32–7.36 (t, 1H, Ar**H**, J=8.3 Hz).

2.2.5. 1-Ethylpropyl (*R*)-2-(3-methyl-4-thiocyanatophenoxy)propionate, II-4. The synthetic procedures for compound II-4 were similar to compound I-5. The product was a yellow oil; yield 56%. ^{1}H NMR ($CDCl_3$): δ (ppm): 0.74–0.92 (m, 6H, CH(CH_2C**H**$_3$)$_2$), 1.49–1.62 (m, 4H, CH(C**H**$_2$CH$_3$)$_2$), 1.63–1.65 (d, 3H, C*HC**H**$_3$, J=6.8 Hz), 2.49 (s, 3H, ArC**H**$_3$), 4.73–4.77 (q, 1H, C***H**COO, J=6.8 Hz), 4.80–4.85 (m, 1H, COOC**H**), 6.74–6.76 (dd, 1H, Ar**H**, J=8.7, 2.8 Hz), 6.84 (d, 1H, Ar**H**, J=2.8 Hz), 7.51–7.53 (d, 1H, Ar**H**, J=8.7 Hz).

2.2.6. 1-Ethylpropyl (*R*)-2-(3-fluoro-4-sulphanylphenoxy)propionate, I-5 [7]. To a solution of the compound I-4 (2.00 g, 6.5 mmol) in absolute ethanol (35 ml), sodium borohydride (0.61 g, 16 mmol) was added dropwise at 0°C. After stirring for 2 h, water (20 ml) was slowly added to the mixture. The ethanol was removed by evaporation, and the residue extracted with ether (50 ml × 3). The combined ether layers were washed with water and dried over anhydrous

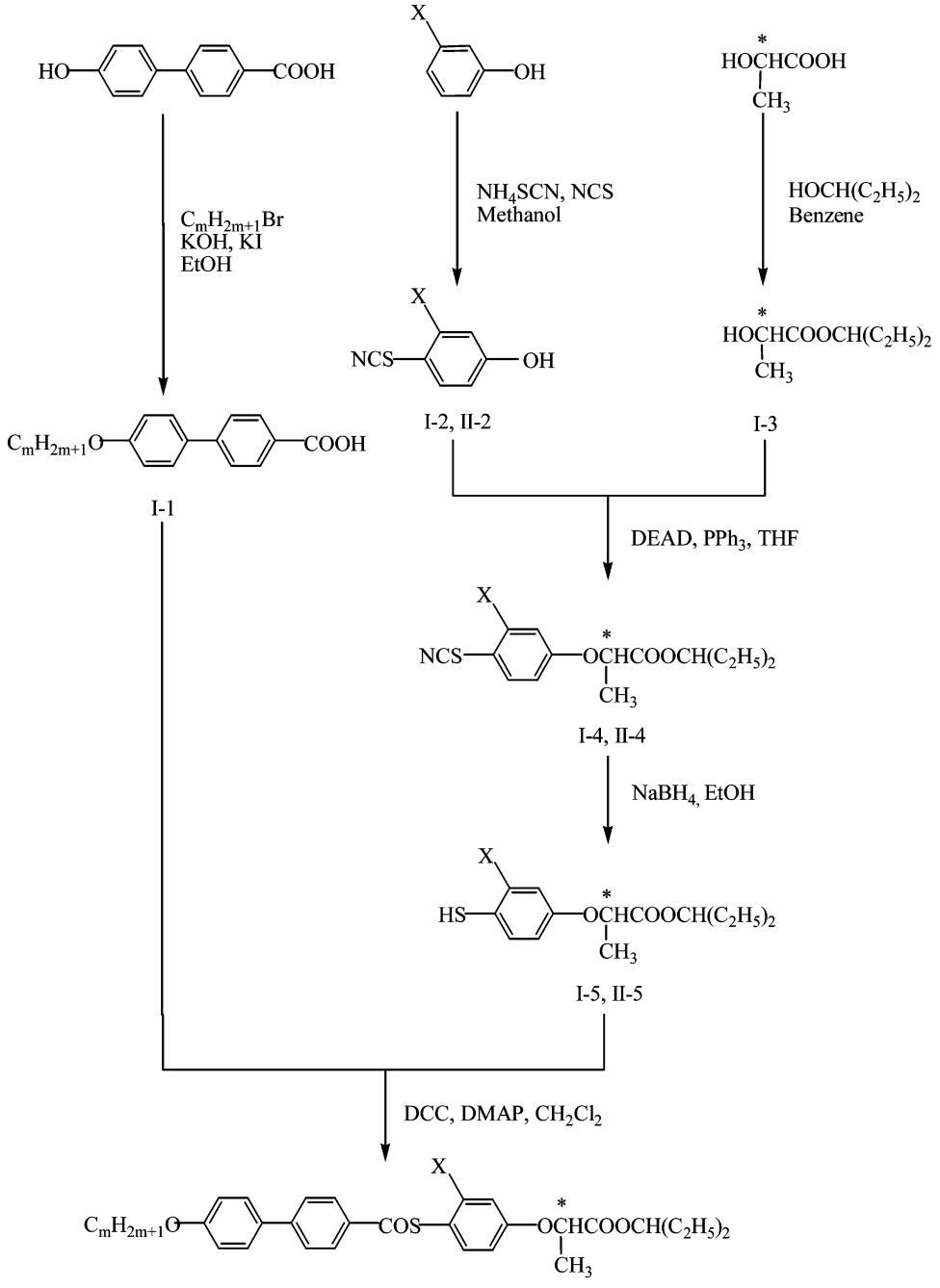

I-6: (m=8-12; X=F)

II-6: (m=8-12; X=CH_3)

Scheme 1. Synthetic procedures for target compounds I-6 (m=8–12; X=F) and II-6 (m=8–12; X=CH_3).

magnesium sulphate. After the removal of ether, the residue was purified by column chromatography on silica gel (70–230 mesh) using dichloromethane as eluant. The product was obtained as a colourless oil; yield 92%. ^{1}H NMR ($CDCl_3$): δ (ppm): 0.75–0.91 (m, 6H, $CH(CH_2C\mathbf{H}_3)_2$), 1.50–1.61 (m, 4H,$CH(C\mathbf{H}_2CH_3)_2$), 1.63–1.64 (d, 3H, C*HC$\mathbf{H}_3$, J=6.8 Hz), 3.36 (s, 1H, Ar**SH**), 4.66–4.70 (q, 1H, C***H**COO, J=6.8 Hz), 4.80–4.83 (m, 1H, COOC**H**), 6.59–6.66 (m, 2H, Ar**H**), 7.18–7.26 (t, 1H, Ar**H**, J=8.6 Hz).

2.2.7. 1-Ethylpropyl (*R*)-2-(3-methyl-4-sulphanylphenoxy)propionate, II-5. The synthetic procedures for compound II-5 were similar to compound I-5. The product was obtained as a colourless oil; yield 95%. ^{1}H NMR ($CDCl_3$): δ (ppm): 0.74–0.91 (m, 6H, $CH(CH_2C\mathbf{H}_3)_2$), 1.49–1.58 (m, 4H, $CH(C\mathbf{H}_2CH_3)_2$), 1.60–1.62 (d, 3H, C*HC$\mathbf{H}_3$, J=6.8 Hz), 2.31 (s, 3H, ArC$\mathbf{H}_3$), 3.12 (s, 1H, ArS**H**), 4.67–4.71 (q, 1H, C***H**COO, J=6.8 Hz), 4.80–4.83 (m, 1H, COOC**H**), 6.61–6.63 (dd, 1H, Ar**H**, J=8.6, 2.8 Hz), 6.74 (d, 1H, Ar**H**, J=2.7 Hz), 7.20–7.22 (d, 1H, Ar**H**, J=8.5 Hz).

2.2.8. 1-Ethylpropyl (*R*)-2-[3-fluoro-4-(4′-alkyloxybiphenylcarbonylthio)phenoxy]propionates, I-6 (m=8–12) [11]. Compound I-6 (m=12) is taken as an example. A solution of compound I-1 (m=12) (0.96 g, 2.5 mmol), compound I-5 (0.59 g, 2.1 mmol), DCC (0.52 g, 2.5 mmol) and DMAP (0.03 g, 0.2 mmol) in dry dichloromethane (30 ml) was stirred at room temperature for two days. The precipitates were filtered off and washed with dichloromethane. The filtrate was successively washed with 5% acetic acid, 5% aqueous sodium hydroxide and water (50 ml × 3), and then dried over anhydrous magnesium sulphate. After removing the solvent, the residue was purified by column chromatography on silica gel (70–230 mesh) using dichloromethane as eluant. The final product was recrystallized from absolute ethanol to give 1-ethylpropyl (*R*)-2-[3-fluoro-4-(4′-alkyloxybiphenylcarbonylthio)phenoxy]propionate as colourless needles; yield 26%. ^{1}H NMR ($CDCl_3$): δ (ppm): 0.78–0.81 (t, 3H, C$\mathbf{H}_3$, J=7.5 Hz), 0.88–0.93 (m, 6H, $CH(CH_2C\mathbf{H}_3)_2$), 1.25–1.64 (m, 18H, $CH_3(C\mathbf{H}_2)$, 1.66–1.67 (d, 3H, C*HC$\mathbf{H}_3$, J=6.8 Hz), 1.78–1.84 (m, 2H, $C\mathbf{H}_2CH_2O$), 4.00–4.02 (t, 2H, $CH_2C\mathbf{H}_2O$, J=6.6 Hz), 4.75–4.79 (q, 1H, C***H**COO, J=6.8 Hz), 4.82–4.87 (m, 1H, COOC**H**), 6.76–6.77 (d, 2H, Ar**H**, J=8.5 Hz), 6.99–7.00 (d, 2H, Ar**H**, J=8.7 Hz), 7.36–7.39 (t, 1H, Ar**H**, J=8.5 Hz), 7.56–7.58 (d, 2H, Ar**H**, J=8.5 Hz), 7.65–7.67 (d, 2H, Ar**H**, J=8.5 Hz), 8.06–8.07 (d, 2H, Ar**H**, J=8.5 Hz).

2.2.9. 1-Ethylpropyl (*R*)-2-[3-methyl-4-(4′-alkyloxybiphenylcarbonylthio)phenoxy]propionates, II-6 (m=8–12). Compound II-6 (m=12) is taken as an example. A solution of the compound I-1 (m=12) (0.9 g, 2.3 mmol), compound II-5 (0.55 g, 2.0 mmol), DCC (0.48 g, 2.3 mmol) and DMAP (0.02 g, 0.2 mmol) in dry dichloromethane (30 ml) was stirred at room temperature for two days. The precipitates were filtered off and washed with dichloromethane. The filtrate was successively washed with 5% acetic acid, 5% aqueous sodium hydroxide and water (50 ml × 3), and then dried over anhydrous magnesium sulphate. After the removal of solvent, the residue was purified by column chromatography on silica gel (70–230 mesh) using dichloromethane as eluant. The final product was recrystallized from the absolute ethanol to give 1-ethylpropyl (*R*)-2-[3-methyl-4-(4′-alkyloxybiphenylcarbonylthio)phenoxy]propionate as colourless needles; yield 32%. ^{1}H NMR ($CDCl_3$): δ (ppm): 0.78–0.81 (t, 3H, C$\mathbf{H}_3$, J=7.5 Hz), 0.88–0.94 (m, 6H, $CH(CH_2C\mathbf{H}_3)_2$), 1.30–1.63 (m, 18H, $CH_3(C\mathbf{H}_2)$,1.64–1.66 (d, 3H, C*HC$\mathbf{H}_3$, J=6.8 Hz), 1.78–1.84 (m, 2H, $C\mathbf{H}_2CH_2O$), 4.00–4.02 (t, 2H, $CH_2C\mathbf{H}_2O$, J=6.6 Hz), 4.76–4.80 (q, 1H, C***H**COO, J=6.8 Hz), 4.82–4.87 (m, 1H, COOC**H**), 6.77–6.79 (dd, 1H, Ar**H**, J=8.5, 2.7 Hz), 6.89 (d, 1H, Ar**H**, J=2.6 Hz), 6.98–7.00 (d, 2H, Ar**H**, J=8.7 Hz) 7.36–7.38 (d, 1H, Ar**H**, J=8.5 Hz), 7.56–7.58 (d, 2H, Ar**H**, J=8.7 Hz), 7.65–7.66 (d, 2H, Ar**H**, J=8.5 Hz), 8.07–8.09 (d, 2H, Ar**H**, J=8.5 Hz).

3. Results and discussion

3.1. *Mesomorphic properties*

Mesophases were identified from observation of texture under the polarizing optical microscope. Transition temperatures and enthalpies for all the materials were determined principally by DSC at a scanning rate of 5°C min^{-1}. In the case of compounds I-6 (m=8–12), the BPII phase was confirmed by the formation of platelet textures. The N* phase was confirmed by the formation of paramorphotic textures; the SmC* phase was characterized by the formation of fan-shaped striated textures. In the case of compounds II-6 (m=8–12), the N* phase was demonstrated by the formation of schlieren textures. The TGBA* phase was confirmed by the formation of spiral filament textures. The SmA* phase was detected by the observation of focal-conic textures in conjunction with homeotropic regions.

The mesophases, transition temperatures, and corresponding phase transition enthalpies for compounds I-6 (m=8–12) and II-6 (m=8–12) are listed in tables 1 and 2, respectively. The phase diagrams of transition temperature plotted against the number of carbon atoms in the achiral chain are shown in figures 1 and 2 for both series of materials. Figure 1 shows that the elongation of achiral aliphatic chain suppresses the formation of the N* phase and favours the formation of the SmC* phase. Therefore, the temperature range of the SmC* phase slightly increases with increasing length of the achiral aliphatic chain. Figure 2 shows that increasing the length of the achiral aliphatic chain enhances the formation of the SmA* phase, but the temperature range of the N* phase, in contrast,

Table 1. Transition temperatures T (°C) and enthalpies ΔH (kJ mol^{-1}) in italics, of materials I-6 (m=8–12) at a cooling rate of 5°C min^{-1}.

m	I		BPII		N*		SmC*		Cr[c]	m.p.[d]
8	•	111.1	•	110.8	•	60.5	•	<−20[b]	—	71.1
		0.80		[a]		*0.15*				*39.77*
9	•	105.9	•	105.4	•	57.5	•	19.6	•	71.3
		0.68		[a]		*0.16*		*21.0*		*38.1*
10	•	106.4	•	106.0	•	62.6	•	<−20[b]	—	68.9
		0.71		[a]		*0.19*				*33.8*
11	•	102.0	•	101.8	•	63.2	•	0.7	•	59.3
		0.73		[a]		*0.21*		*15.1*		*29.8*
12	•	101.7	•	101.4	•	67.2	•	0.9	•	48.2
		0.92		[a]		*0.14*		*14.3*		*28.1*

[a]The enthalpy of the BP_{II}–N* transition was added with that of the I–BP_{II} transition.
[b]The crystal phase temperature is below −20°C.
[c]Cr refers to the crystal phase.
[d]m.p. refers to the melting point taken from DSC thermograms recorded at a heating rate of 5°C min^{-1}.

Table 2. Transition temperatures T (°C) and enthalpies ΔH (kJ mol^{-1}) in italics, of materials II-6 (m=8–12) at a cooling rate of 5°C min^{-1}.

m	I		N*		TGBA*		SmA*		Cr*	m.p.[d]
8	•	99.7	•	68.8	•	63.2	•	<−10[b]	—	80.8
		0.73		*0.23*		[a]				*28.9*
9	•	94.7	•	65.8	•	57.7	•	<−10[b]	—	66.9
		1.67		*0.37*		[a]				*26.6*
10	•	92.9	•	67.4	•	60.6	•	<−10[b]	—	52.3
		0.79		*0.15*		[a]				*28.6*
11	•	90.0	•	69.3	•	62.7	•	13.3	•	55.3
		0.80		*0.50*		[a]		*14.4*		*30.4*
12	•	90.4	•	76.2	•	71.5	•	−3.8	•	51.0
		0.86		*0.33*		[a]		*13.5*		*27.0*

[a]The enthalpies were too small to be measured.
[b]The crystal phase temperature is below −10°C.
[c]Cr refers to the crystal phase.
[d]m.p. refers to the melting point taken from DSC thermograms recorded at a heating rate of 5°C min^{-1}.

decreases. The melting points of the two series of compounds are similar, but the clearing temperatures of the II-6 (m=8–12) are much lower than those of the I-6 (m=8–12), suggesting that the methyl group could lower the clearing points due to a steric effect. In addition, the methyl group suppresses the formation of the SmC* phase but instead generates a TGBA* phase.

3.2. *Spontaneous polarization*

The spontaneous polarization ($\mathbf{P}_s$) was calculated by integration of the switching current under a triangular wave at 20 Hz. The amplitude of the triangular wave was 5 V, which was sufficient to unwind the helical structure. The spontaneous polarizations for I-6 (m=10–12) were measured in the temperature range of the SmC* phase, and the temperature dependency of spontaneous polarization is illustrated in figure 3. The $\mathbf{P}_s$ values depend on temperature and exhibit maximum values of about 91–95 nC cm^{-2}.

3.3. *Apparent tilt angle*

The apparent tile angle θ was measured using the same field and frequency as for the polarization measurements, using the usual 2θ optical method [12]. The apparent tilt angle was measured in 5 μm homogeneously aligned cells. Figure 4 shows that when lowering the temperature to the SmC* phase via a first-order phase transition [13] the tilt angles of compounds I-6 (m=10–12) start at a point greater than zero and finally have constant tilt angles about 34–37°.

3.4. *Dielectric properties*

The temperature dependence of the dielectric constant ε' was measured at 100 Hz in 25 μm homogeneously

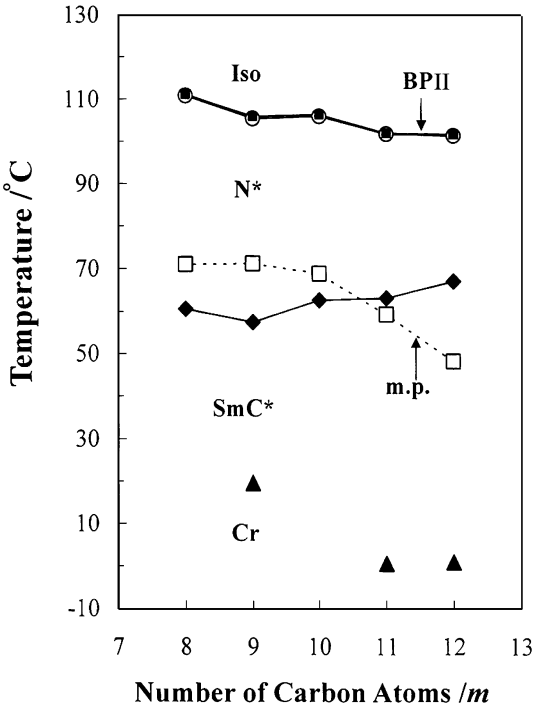

Figure 1. Plot of transition temperature as a function of achiral terminal aliphatic chain length (m) for compounds I-6 (m=8–12) during cooling.

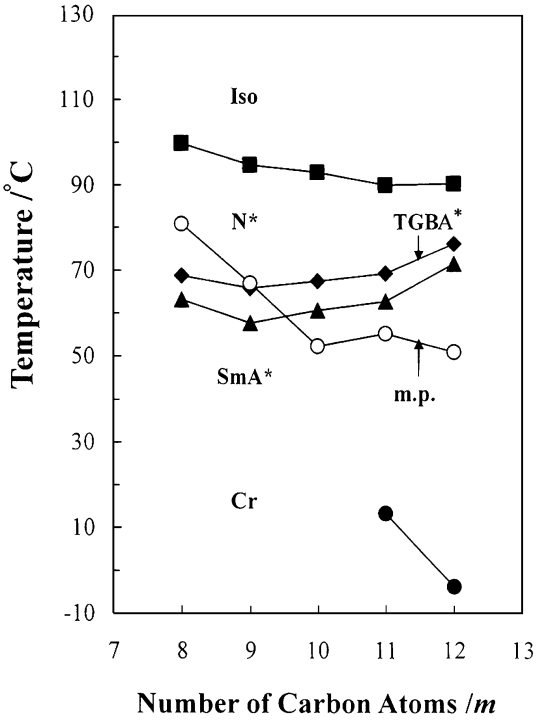

Figure 2. Plot of transition temperature as a function of achiral terminal aliphatic chain length (m) for compounds II-6 (m=8–12) during cooling.

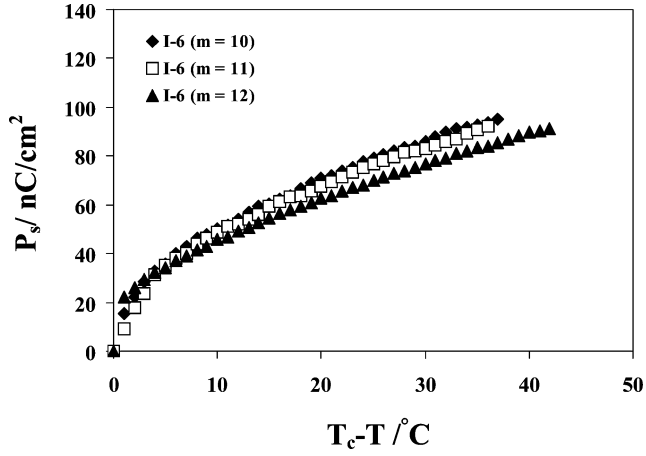

Figure 3. Spontaneous polarization plotted as a function of temperature for I-6 (m=10–12). T_c is the temperature of the N*–SmC* phase transition.

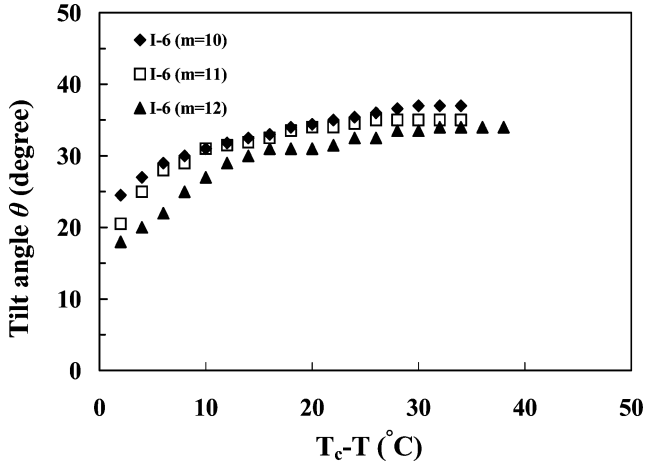

Figure 4. Tilt angle versus temperature for I-6 (m=10–12) below the N*–SmC* phase transition in a 5 µm thick cell. T_c is the temperature of the N*–SmC* phase transition.

aligned cells, with results depicted in figure 5. The scanning rate is kept at 0.5°C min^{-1}. The ε' values in the N* phase are small; with decreasing temperature, the ε' slightly increases at the N*–SmC* phase transition. On cooling to the SmC* phase, the dielectric constants increase sharply, due to the contribution of the Goldstone mode [14].

4. Conclusion

Two structurally similar chiral swallow-tailed thioester materials, I-6 (m=8–12) and II-6 (m=8–12), with different substitutions (X=F or CH_3) on the phenyl ring of the rigid core, have been investigated. The results show that materials I-6 (m=8–12) having a fluoro substituent exhibit a ferroelectric SmC* phase

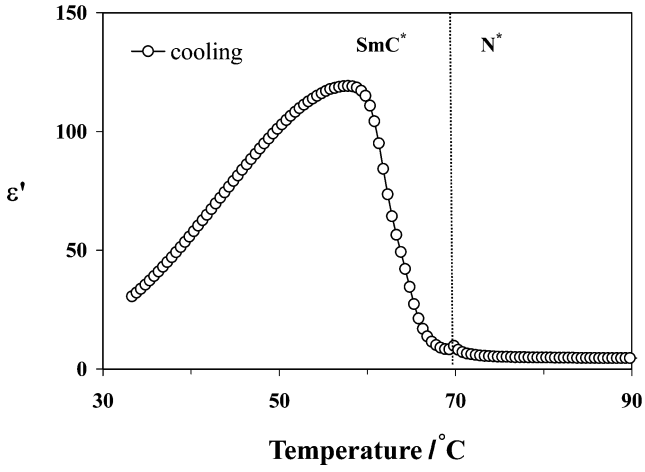

Figure 5. Temperature dependence of the dielectric constant ε' for I-6 (m=12) at 100 Hz in a 25 µm thick cell during cooling at 0.5°C min^{-1}.

that encompass room temperature; however, most of them are monotropic. In materials II-6 (m=8–12) having a methyl substituent, SmC* phase formation is suppressed, demonstrating that the methyl group at the 3-position of the phenyl ring prohibits molecular tilted pairing due to a steric effect. This steric effect also results in the formation of the TGBA* phase at the transition from the N* to SmA* phase. In addition, the materials with the methyl substituent, in general, have lower phase transition temperatures than corresponding materials with the fluoro subtituent.

References

[1] D.J. Byron, L. Komitov, A.S. Matharu, I. McSherry, R.C. Wilson. *J. mater. Chem.*, **6**, 1871 (1996).
[2] L. Nassif, A. Jakli, A.J. Seed. *Mol. Cryst. liq. Cryst.*, **365**, 171 (2001).
[3] A.J. Seed, M. Hird, P. Styring, H.F. Gleeson, J.T. Mills. *Mol. Cryst. liq. Cryst.*, **299**, 19 (1997).
[4] A.J. Seed, K.J. Toyne, J.W. Goodby, D.G. McDonnell. *J. mater. Chem.*, **5**, 1 (1995).
[5] M.E. Neubert, R.E. Cline, M.J. Zawaski, A. Ekachai. *Mol. Cryst. liq. Cryst.*, **76**, 43 (1981).
[6] M.E. Neubert, B.Z. Merchant, M.R. Jirousek, S.J. Laskos, D. Leohardt, R.B. Sharma. *Mol. Cryst. liq. Cryst.*, **154**, 209 (1988).
[7] H. Okamoto, J.-W. Wu, Y. Morita, S. Takenaka. *Bull. chem. Soc. Jpn.*, **75**, 175 (2002).
[8] P.J. Collings, M. Hird. *Introduction to Liquid Crystals*, p. 70, Taylor and Francis Ltd., Hong Kong (1997).
[9] S.-L. Wu, C.-Y. Lin. *Liq. Cryst.*, **290**, 1575 (2002).
[10] K. Miyasato, S. Abe, H. Takezoe, A. Fukuda, T. Kuze. *Jpn. J. appl. Phy.*, **22**, L661 (1983).
[11] C.J. Booth, A. Dunnur, J.W. Goodby, K.J. Toyne. *Liq. Cryst.*, **28**, 815 (1996).
[12] P. Martinot-Lagarde, R. Pindak, G. Durand. *Mol. Cryst. liq. Cryst.*, **75**, 249 (1981).
[13] J.W. Goodby, R. Blinc, N.A. Clack, S.T. Lagerwall, M.A. Osipov, S.A. Pikin, T. Sakurai, K. Yoshino, B. Žekš. Ferroelectric Liquid Crystals p3, Gorbon and Breach Science Publishers, Philadelphia, (1991).
[14] (*a*) J.W. Goodby, R. Blinc, N.A. Clack, S.T. Lagerwall, M.A. Osipov, S.A. Pikin, T. Sakurai, K. Yoshino, B. Žekš. Ferroelectric Liquid Crystals p6, Gorbon and Breach Science Publishers, Philadelphia, (1991). (*b*) M. Cepic, G. Heppke, J.M. Hollidt, D. Lotzsch and B. Beks. *Ferroelectrics*, **147**, 179 (1994).